Design of a β-hairpin peptide-intercalator conjugate for simultaneous recognition of single stranded and double stranded regions of RNA†

Lauren L. Cline and Marcey L. Waters*

Received 2nd July 2009, Accepted 3rd August 2009
First published as an Advance Article on the web 2nd September 2009
DOI: 10.1039/b913024a

Designing receptors that bind RNA is a challenging endeavor because of the unique and sometimes complex structure of RNA. However these structural features provide regions for ligands to bind using different types of interactions. To increase specificity and binding affinity to RNA, divalent systems have been designed which incorporate more than one binding motif into one molecule. Using this approach, we have designed a two part heteroconjugate, **WKWK-Int**, which contains a β-hairpin peptide covalently linked to an RNA intercalator. This heteroconjugate was designed to bind duplex RNA through intercalation and simultaneously interact with a single stranded bulge region using the side chains of the β-hairpin peptide. We have used fluorescence anisotropy experiments to show that the heteroconjugate has an increased binding affinity over either one of the individual ligands. Additionally, RNase footprinting experiments show that the structure of the peptide is necessary for the protection of one particular base in the RNA bulge region. When tested against other RNA molecules containing a stem-bulge structure, the designed heteroconjugate was found to be specific for this RNA sequence. This work provides evidence that the covalent linkage of two weak RNA ligands can greatly increase the binding affinity and also provide specificity to the binding event.

Introduction

In recent years, RNA has gained significant attention as a potential medicinal target.[1] However, designing ligands that bind RNA has proven to be a challenging endeavor. This is in part due to its unique and sometimes complex structure, including regions of single and double stranded RNA, loops, bulges, and tertiary interactions. Nonetheless, these structural features of RNA provide regions for ligands to bind using different types of interactions, including intercalation, stem binding through electrostatic and hydrogen bonding interactions, and loop or bulge binding utilizing aromatic stacking interactions in addition to hydrogen bonding and electrostatic interactions. For example, many RNA-protein structures show that recognition occurs at single stranded regions of RNA through a combination of aromatic, electrostatic, and hydrogen bonding interactions.[2] Several different types of synthetic molecules have been explored for binding to RNA[1] such as aminoglycosides,[3] polyamines,[4] deoxystreptamine dimers,[5] peptidomimetics,[6] peptides,[7] and small intercalating agents.[8] Some of these have been found to have high affinity for RNA, but high specificity has proven difficult to achieve.

To increase affinity and selectivity, several groups have combined two different types of RNA binders to obtain heteroconjugates that target two different structural features of RNA. These include combinations of aminoglycosides for groove binding, intercalators for stem binding, cationic peptides for electrostatic binding to the RNA backbone, and small molecules or peptide nucleic acids (PNAs) for loop binding. For example, Tor and coworkers found an approximately 20-fold enhancement in binding of a neomycin-acridine heteroconjugate to RRE relative to neomycin alone, giving an inhibitor with a binding affinity equivalent to that of the REV-RRE interaction.[9] This work was expanded to show what importance linker length and the type of aminoglycoside has on RNA binding.[10] Teulade-Fichou and coworkers also used an aminoglycoside-quinacridine intercalator conjugate and found that it bound well to telomerase RNA.[11] Several groups have explored combinatorial libraries of aminoglycoside-peptide conjugates for RNA binding,[12] and others have found that just the addition of arginine to an intercalator or aminoglycoside can improve binding and specificity to TAR RNA.[13] The Yu group has also explored a number of heteroconjugates, including aminoglycosides with peptide nucleic acids or small molecules that are known to bind loop regions.[14] In addition, the Yu group has designed cationic α-helical peptides with aromatic and/or intercalating groups as multivalent binders.[15]

Our group has previously designed a well-folded β-hairpin peptide that binds to single-stranded regions of DNA *via* aromatic stacking and electrostatic interactions.[16] Thus, we envisioned that this structured peptide may provide a new approach for targeting loops and/or bulges with unstacked bases. To provide additional affinity and selectivity, we chose to conjugate the β-hairpin to an intercalator that exhibits a preference for binding near internal bulges.

A conjugated system was designed that contains an RNA intercalator connected to a well-folded β-hairpin peptide through a flexible linker, **WKWK-Int** (Fig. 1a). The β-hairpin peptide targets unpaired bases in the single stranded regions of RNA, while the intercalator orients the complex by binding a specific site in the

Department of Chemistry, The University of North Carolina at Chapel Hill, CB 3290, Chapel Hill, NC 27599. E-mail: mlwaters@email.unc.edu; Fax: +1 919 962 2388; Tel: +1 919 843 6522

† Electronic supplementary information (ESI) available: Structures and footprinting assays of control peptides, CD spectra, and mass spectral data. See DOI: 10.1039/b913024a

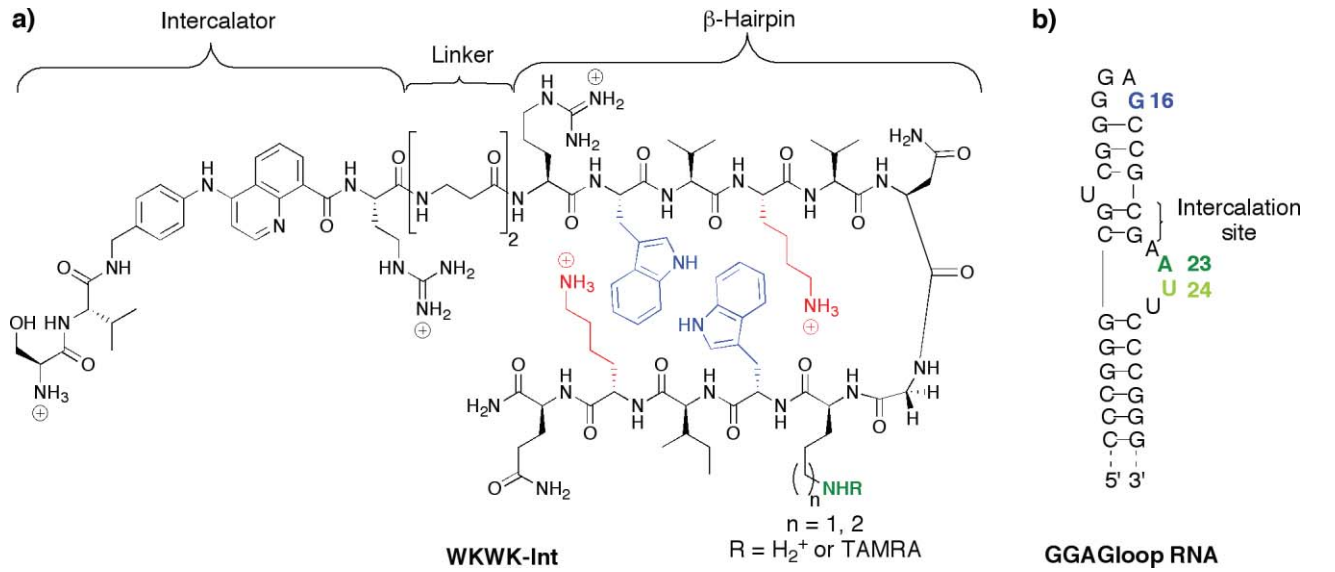

Fig. 1 Structure and sequence of (a) **WKWK-Int** and (b) **GGAGloop RNA**. (a) The nucleotide binding pocket in **WKWK-Int**, is colored blue and red, and the position for attachment of the fluorophore is green. (b) Bases in which protection was observed in the loop and bulge are indicated in color.

duplex RNA region. The two pieces utilize different methods for binding RNA, and by connecting them together we gained a more selective system with a tighter binding affinity. To our knowledge, this is the first example of an RNA binding molecule which combines a β-hairpin peptide with a sequence selective RNA intercalator.

Results and discussion

Peptide and RNA design

The β-hairpin portion of **WKWK-Int** is based on the previously reported WKWK peptide named for the four residues that make up a binding cleft for nucleotides on one face of the hairpin. As a monomer this peptide has a modest binding affinity for ATP (K_d = 170 μM)[17] and as a dimer it binds well to single stranded DNA (K_d = 3 μM).[16] This peptide has been characterized by NMR to be 95% folded in aqueous environment.[16,17] Mutation studies indicate that ATP interacts with the two tryptophan residues through π-π stacking and electrostatic interactions are made with the lysine side chains. This peptide was chosen because it will be able to bind to solvent exposed bases in the loop and bulge regions of RNA.

For the intercalator portion of **WKWK-Int** we used the quinoline-based RNA intercalator developed by Beal and coworkers to bind double stranded regions of RNA.[18] This intercalator has been found to preferentially thread between two G-C base pairs which are directly adjacent to bulge sites. The Beal group synthesized a small five residue peptide, AbuSV*Quin*R, which contained this intercalator as an unnatural amino acid. Footprinting experiments found that it bound to a specific RNA sequence with low micromolar affinity. This particular intercalator was chosen due to its site specificity and ease of incorporation into peptide synthesis.

The two pieces were connected using a βAla-βAla linker, which is both flexible and can provide additional points of hydrogen bonding interactions. During early studies the heteroconjugate was synthesized with one, two, or three β-alanines linking the two pieces. Initial results suggested that a heteroconjugate with a single residue linker did not bind as well as those made with two and three β-Ala residues, which both had comparable binding.[19] For ease of synthesis and to eliminate additional entropic costs of using a longer linker, all subsequent heteroconjugates were made with a two residue linker.

Control peptides were also designed to help investigate the structure-activity relationship for **WKWK-Int** (Fig. S1, supplemental information). The **Int-control** peptide contains the intercalator and linker regions only, while the **WKWK-control** contains the β-hairpin peptide and linker regions alone. Two additional controls were designed to determine the influence of the peptide structure on RNA binding. The **GKGK-Int** control was designed to have all the amino acids in the β-hairpin portion replaced with glycine except the charged residues. This gives **GKGK-Int** the same charge state as **WKWK-Int**, but it lacks secondary structure. The **GWKWKG-Int** control peptide was designed to have glycines replace all the residues except the charged residues and the aromatic tryptophan residues. This control peptide is also unstructured because it lacks an Asn-Gly turn sequence and key side chain-side chain interactions, but it has the same charge state as **WKWK-Int** and the ability to make aromatic interactions. Circular dichroism (CD) studies confirmed that **GKGK-Int** and **GWKWKG-Int** are unstructured, whereas **WKWK-Int** takes on a β-hairpin structure (Fig. S2, supplemental information).

The RNA sequence chosen for these experiments contains regions of both double stranded and single stranded bases making it suitable for binding both parts of **WKWK-Int** (Fig. 1b). The sequence, **GGAGloop RNA**, contains a single stranded GGAG hairpin loop that was chosen because of its biological relevance in the SL3 Ψ-RNA recognition element of the HIV-1 nucleocapsid protein and because the published NMR structure shows that three of the four residues are unstacked.[20] The rest of the RNA sequence mimics one used by the Beal group, which contains a single stranded internal 5′-AAUU-3′ bulge that may include

Table 1 Binding dissociation constants as measured by fluorescence anisotropy with TAMRA-labeled peptides[a]

Peptide	K_d (μM)
WKWK-Int	3.7 ± 0.7
GKGK-Int	9.7 ± 2.2
GWKWKG-Int	31.8 ± 13.1
WKWK-control	>100
Int-control	>100

[a] Experiments were done with 0.5 μM peptide in 10 mM PBS buffer (140 mM Na^+/K^+Cl^-, 1 mM $MgCl_2$, pH 7.4) at 25 °C. Error is the standard deviation of an average of 3 or 4 runs.

solvent exposed bases.[18] This bulge region and an additional 5′-U bulge flank the two G-C base pairs where the intercalator molecule threads upon binding.

Binding assays with GGAGloop RNA

Fluorescence anisotropy experiments were performed to find the dissociation constant (K_d) of **WKWK-Int** binding to the RNA and compare that to the dissociation constants for the **Int-control**, **WKWK-control**, **GKGK-Int**, and **GWKWKG-Int**. The peptides were labeled with 5(and-6)-carboxytetramethylrhodamine (TAMRA) fluorophore through a lysine side chain on the opposite face of the WKWK binding pocket (Fig. 1). It has been shown that altering this side chain does not affect the structure or stability of the peptide.[21]

The fluorescence experiments indicate that **WKWK-control** and **Int-control** peptides do not measurably bind to the RNA (Fig. 2, Table 1). However when the two pieces are connected in **WKWK-Int**, the binding affinity greatly increases (K_d = 3.7 ± 0.7 μM). The unstructured **GKGK-Int** binds to the RNA with three-fold lower binding affinity (K_d = 9.7 ± 2.2 μM) and the **GWKWKG-Int** binds with a dissociation constant of 31.8 ± 13.1 μM. This suggests that although electrostatic interactions are driving the binding there is some increased binding due to either the β-hairpin structure or specific contact with non-charged

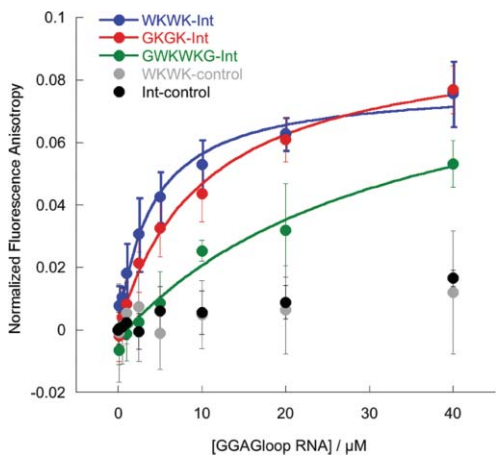

Fig. 2 Fluorescence anisotropy binding experiments of TAMRA-labeled heteroconjugates with **GGAGloop RNA**; **WKWK-control** (gray), **Int-control** (black), **WKWK-Int** (blue), **GKGK-Int** (red), and **GWKWKG-Int** (green). Experiments were done with 0.5 μM peptide in 10 mM PBS buffer (140 mM Na^+/K^+Cl, 1 mM $MgCl_2$, pH 7.4) at 25 °C and each curve is an average of 3 or 4 runs. Data were fit using eqn (1).

side chains. The fact that **GWKWKG-Int** is a weaker binder than **GKGK-Int** suggests that the Trp residues in this unstructured peptide may somehow prohibit optimal electrostatic interactions between the positively charged residues on the peptide and the phosphate backbone of the RNA, perhaps through intramolecular cation-π interactions.

RNase footprinting assays with GGAGloop RNA

Enzymatic footprinting experiments were performed to identify which regions of the RNA make contacts with the heteroconjugates. The **GGAGloop RNA** sequence was 3′-labeled with ^{32}pCp, and enzymatic digestions were performed with RNases that target single stranded regions of RNA (RNase T1 and RNase 1) and double stranded regions of RNA (RNase V1). For these experiments, peptides without the TAMRA fluorophore were used, such that the net charge on each peptide is greater by +1 than those used for fluorescence anisotropy (Fig. 1). These experiments helped to identify whether contacts were being made in the hairpin loop region (bases G13-G16), the bulge region (bases A22-U25), or the stem region.

The footprinting experiments show that **WKWK-Int** specifically protects residue G16 in the loop, A23 and U24 in the bulge, and much of the double stranded stem region around the expected intercalation site (Figs. 3a and 3b). These experiments provide evidence that **WKWK-Int** binds the RNA in several different regions simultaneously. Neither **Int-control** nor **WKWK-control**, which only contain one binding motif, measurably binds **GGAGloop RNA** (Figs. S3 and S4, supplemental information). This is consistent with the fluorescence anisotropy data confirming that both portions of the heteroconjugate are needed for binding.

Both **GKGK-Int** and **GWKWKG-Int** make similar contacts in the hairpin loop and stem regions as **WKWK-Int** (Fig. 3 and Fig. S5, supplemental information). However, experiments done with RNase 1 show that the cleavage pattern differs in the bulge region. **WKWK-Int** protects residue A23 from RNase 1 cleavage, whereas **GKGK-Int** provides no protection for this residue. **GKGK-Int** has the same charge as **WKWK-Int** but lacks structure and an aromatic cleft, suggesting that folding and/or aromatic interactions are needed for binding to A23. **GWKWKG-Int**, which is also unstructured but has the ability to make aromatic interactions, protects the A23 site but to a lesser degree than **WKWK-Int**. These results are consistent with a specific interaction between the folded β-hairpin of **WKWK-Int** and A23 that is weakened when the peptide is unstructured and lost when the aromatic residues are removed.

The intensity of bands G16, A23, and U24 were quantified using ImageQuant software and plotted *versus* the concentration of heteroconjugate (Fig. 4). The data were fit using eqn (1) (see Experimental section), and local binding affinities were determined for each of the bases (Table 2). The local binding affinities measured in this way are consistent with the binding affinities measured *via* fluorescence anisotropy, suggesting that the difference in charge of the TAMRA-labeled and unlabeled heteroconjugates does not significantly influence binding.

The quantitative analysis confirms that **WKWK-Int** binds more tightly to A23 than **GWKWKG-Int** or **GKGK-Int**, which exhibits no binding to A23. There is also evidence that **WKWK-Int** binds to

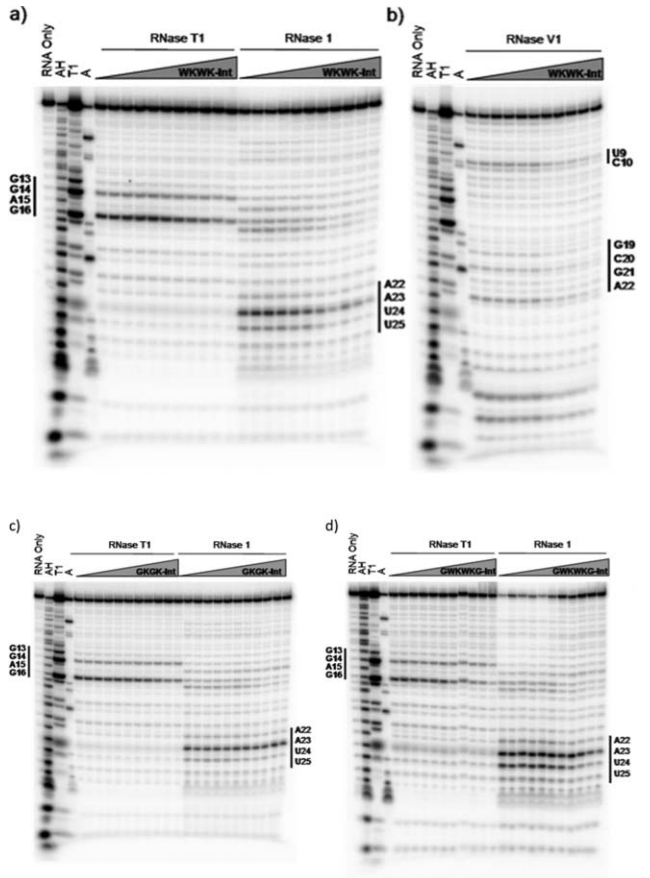

Fig. 3 RNase footprinting experiments of **GGAGloop RNA** with **WKWK-Int** (a and b), **GKGK-Int** (c), and **GWKWKG-Int** (d). Shown is the phosphorimage of a 20% denaturing polyacrylamide gel. Structure lanes: RNA only, folded RNA in buffer; AH, alkaline hydrolysis; T1, RNase T1 (G-lane); A, RNase A (C and U lane). Increasing concentrations (0 to 100 μM) of **WKWK-Int** (a and b) were added to **GGAGloop RNA** (0.18 μM) in 10 mM PBS buffer (140 mM Na^+/K^+Cl^-, 1 mM $MgCl_2$, pH 7.4) and 5 ng/μL yeast tRNA. RNase T1 (cleaves G residues) was used to visualize the G-rich loop region and RNase 1 (cleaves ssRNA) was used to visualize both the loop and internal bulge regions. Bases G14 and G16 were the major cleavage sites for RNase T1, whereas bases A23 and U24 were the major cleavage sites for RNase 1. RNase V1 (cleaves dsRNA) was used to visualize the stem regions of the RNA. Single stranded RNase footprinting experiments for **GKGK-Int** (c) and **GWKWKG-Int** (d) with **GGAGloop RNA**.

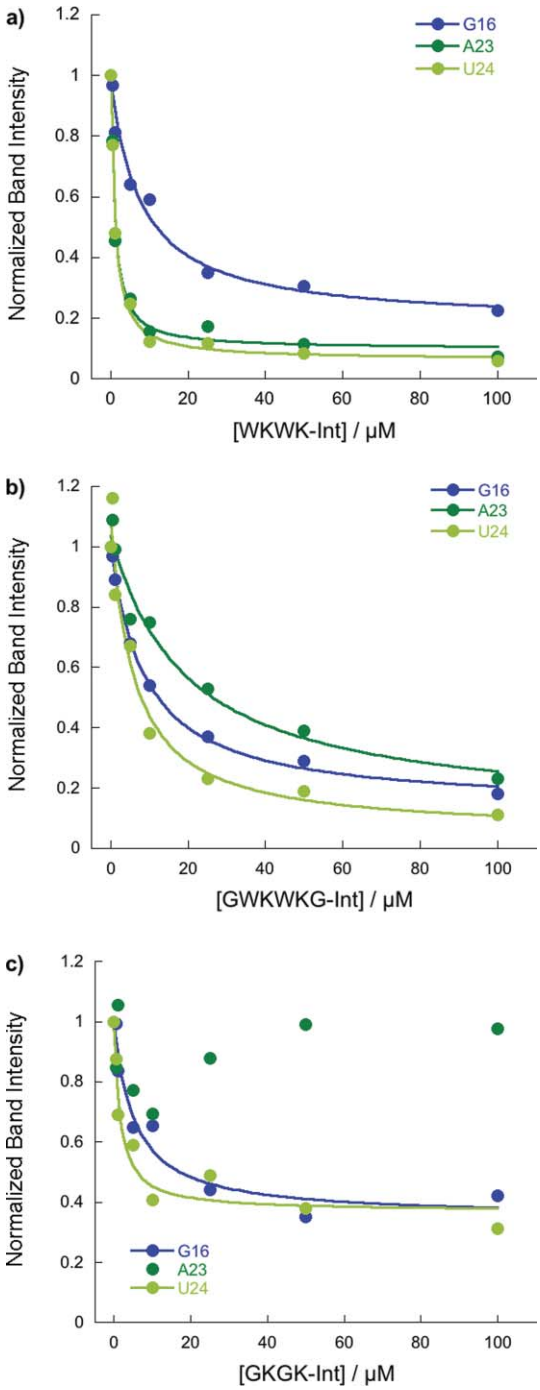

Fig. 4 ImageQuant analysis of RNase footprinting assays showing the degree of protection at G16 (blue), A23 (dark green), and U24 (light green). (a) **WKWK-Int**; (b) **GWKWKG-Int**; (c) **GKGK-Int**.

the bulge more strongly than to the loop region. The local binding affinities indicate that **GWKWK-Int** is a weaker binder than either **WKWK-Int** or **GKGK-Int** at positions G16 and U24, but that it protects A23 to some extent, whereas **GKGK-Int** does not.

In summary, the RNase footprinting experiments show that **WKWK-Int** interacts strongly with the internal bulge region (residues A23 and U24) and moderately with the hairpin loop region (residue G16). Neither **GKGK-Int** nor **GWKWKG-Int** protects the A23 residue as well as **WKWK-Int**, indicating that the structure of the peptide is important for protection of that base. The complete loss of protection of A23 with **GKGK-Int** but not with **GWKWKG-Int** suggests that specific aromatic contacts are made with A23. Because the residue is located in the single stranded bulge, the base may be exposed and able to bind the aromatic pocket of the peptide. This hypothesis is supported by structural data for a similar adenine-rich bulge.[22]

Selectivity studies of WKWK-Int with GGAGloop RNA

All of the footprinting experiments were done in the presence of equimolar amounts of unlabeled yeast tRNA to slow down the enzymatic degradation of the target RNA. It was observed that the dissociation constants are consistent with those found with fluorescence anisotropy where tRNA was not present. We

Table 2 Comparison of local binding affinities for the peptide-intercalator heteroconjugates binding to **GGAGloop RNA**[a]

	K_d/μM (± error)[b]		
Peptide	G16	A23	U24
WKWK-Int	7.8 (2.3)	0.9 (0.2)	1.0 (0.2)
GWKWKG-Int	8.8 (1.0)	19.6 (6.9)	6.0 (2.6)
GKGK-Int	5.2 (2.3)	n.b.[c]	1.6 (0.8)
RevWKWK-Int	6.8 (1.8)	1.5 (0.5)	0.7 (0.1)

[a] Local binding affinities were determined by quantifying the radioactive counts in each band using ImageQuant software, and fitting the data using equation 1 in the Experimental section. [b] Error in dissociation constants was determined using two separate footprinting experiments. [c] No binding detected.

Table 3 Dissociation constants for the different peptide-intercalator conjugates binding to the **GGAGloop RNA** and **GGAGext RNA**[a]

Peptide-intercalator	RNA Sequence	K_d (μM) (± error)[b]
WKWK-Int	GGAGloop RNA	3.7 (0.7)
WKWK-Int	GGAGext RNA	9.7 (2.2)
GKGK-Int	GGAGloop RNA	9.9 (1.3)
GKGK-Int	GGAGext RNA	25.6 (5.1)

[a] As determined by fluorescence anisotropy binding experiments using TAMRA-labeled peptide-intercalator conjugates. Binding constants were determined by fitting the data to eqn (1) in the Experimental section. [b] Error was determined from the standard deviation of 3 to 4 separate experiments.

also investigated the binding of **WKWK-Int** to BIV TAR RNA sequence which contains similar regions of double stranded and single stranded RNA and observed no significant binding (K_d > 100 μM, Fig. S6, supplemental information). These results suggest excellent selectivity for **WKWK-Int** binding to the target RNA.

Investigation of WKWK-Int with reversed orientation

To determine whether there is a preference for which terminus of the intercalator threads the RNA, as has been seen in other cases,[18,23] we designed a heteroconjugate, **RevWKWK-Int** (Fig. 5a) in which the intercalator and the β-hairpin have been switched, so that the intercalator is on the C-terminus and the β-hairpin is on the N-terminus. The results from footprinting experiments show that the same regions of the RNA are protected from RNase cleavage for **RevWKWK-Int** as are for **WKWK-Int** (Fig. 5b). Analysis of the protected regions showed that the local dissociation constants for the internal bulge bases A23 and U24 are 1.5 (± 0.5) μM and 0.7 (± 0.1) μM, respectively, and the dissociation constant for G16 in the hairpin loop was 6.8 (± 1.8) μM (Fig S7 and Table 1). These local binding affinities are within error of the binding affinities determined for **WKWK-Int** with **GGAG RNA**. Thus, it appears that in this system the intercalator can thread either direction and prefers to place the β-hairpin in a position to bind A24 (Fig. 5c). This is unlike Beal's threading intercalator,[18] which selectively places the N-terminus in the minor groove and the C-terminus in the major groove.

Studies using an extended length RNA

The footprinting studies described above show that **WKWK-Int** binds strongly to the internal AAUU bulge region of **GGAGloop RNA**, but that somewhat weaker binding also occurs in the hairpin loop region. To isolate the binding to the bulge region, the RNA sequence was extended in length so that the hairpin loop region would be farther away from the intercalation site (Fig. 6a). The extended RNA, **GGAGext RNA**, makes it impossible for the heteroconjugates to interact with the hairpin loop region, and therefore eliminates any binding in that region. The footprinting experiments with the **GGAGext RNA** confirm that for **WKWK-Int** there is no longer binding in the hairpin loop region, but the interaction in the bulge region remains the same (Fig. 6b). The local dissociation constants for bases A27 and U28 are 2.9 (± 1.7) μM and 2.4 (± 2.2) μM, respectively, which are similar to the binding affinities of **WKWK-Int** for A23 and U24 in the **GGAGloop RNA**. However, fluorescence anisotropy binding experiments show that loss of binding to the loop region results in a lower global binding affinity. Both **WKWK-Int** and the unstructured **GKGK-Int** have a three-fold lower binding affinity for the **GGAGext RNA** (Fig. 7, Table 3).

Conclusions

We have designed a peptide-intercalator conjugate that recognizes RNA by interacting with both the double stranded stem region and single stranded bulge region simultaneously. The binding data indicate that both the intercalator and the peptide portion of the heteroconjugate are required for low micromolar binding to occur; the binding affinity is at least 30-fold more favorable for the heteroconjugate relative to the intercalator or hairpin alone. This system provides an example of how two site-selective ligands with low affinity for a substrate can together create a tighter binding system with high selectivity for the target RNA. This dual-mode method of binding creates a system that is specific for two types of structure, and has been demonstrated to be a viable way of providing specificity for RNA binding molecules, which has been an ongoing challenge. In addition, we have demonstrated the significance of the folding of the hairpin in providing protection to a specific base, likely through aromatic interactions. α-Helical peptides have also recently been shown to act as excellent scaffolds for the display of multiple RNA-binding motifs, which demonstrates the potential of such pre-organized scaffolds in selective RNA binding.[15] This is one of only a few examples of a multivalent RNA binding motif that interacts with two specific structural elements on the RNA simultaneously to provide both increased affinity and selectivity. Through combinatorial screens we aim to optimize the binding affinity and selectivity for biologically relevant RNA structures.

Experimental

Synthesis of the TAMRA-labeled intercalator-peptide conjugates

The intercalator portion, 4-(4′-methylaminoallyoxycarbamate)-aniline-quinoline-8-carboxylic acid, was synthesized following the previously published procedure by Krishnamurthy *et al.*[18] The peptide portions were synthesized on FMOC-PAL-PEG-PS

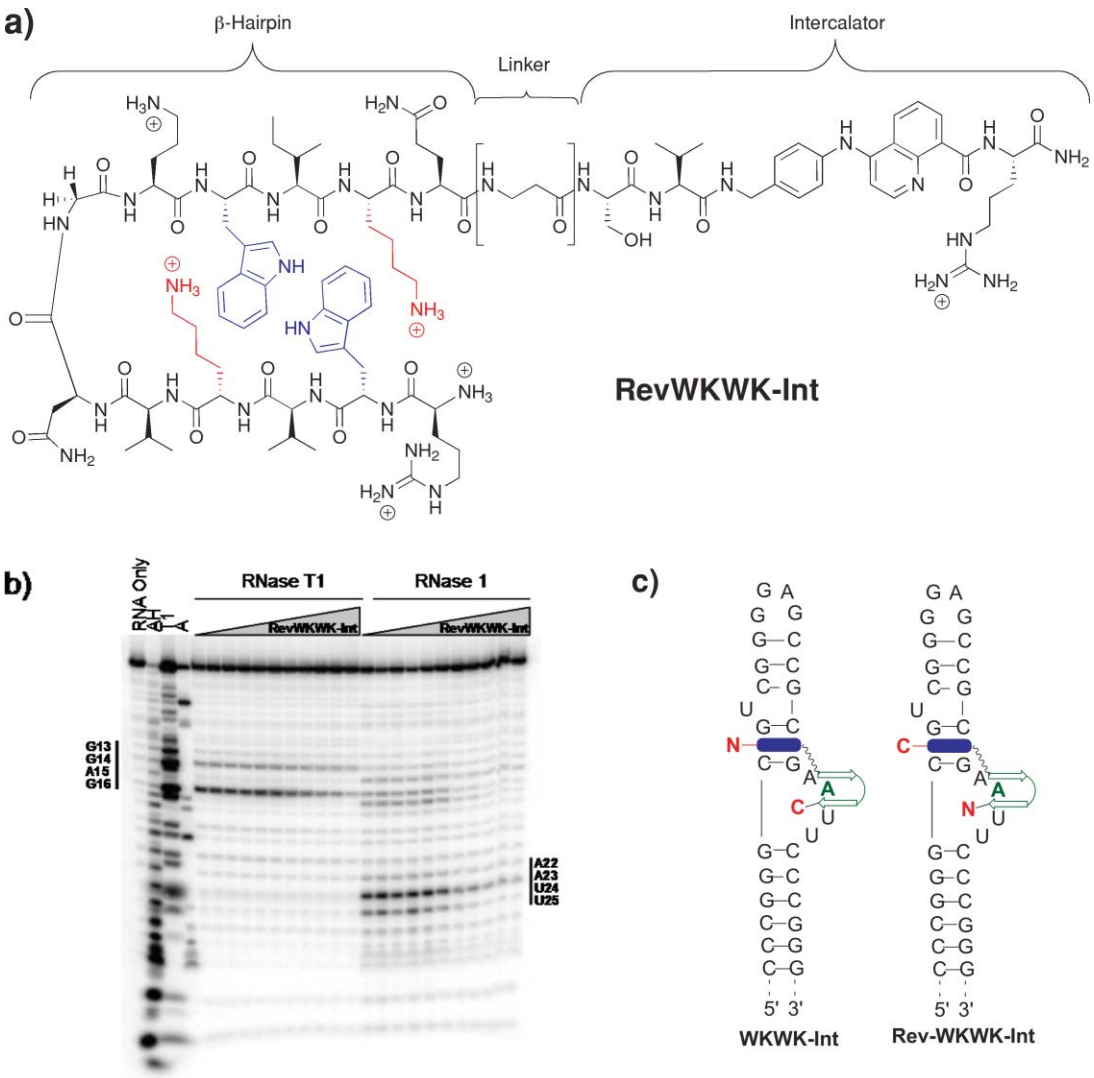

Fig. 5 RNase footprinting experiments of **RevWKWK-Int** with **GGAGloop RNA**. (a) Structure of **RevWKWK-Int**. (b) RNase footprinting experiments for **RevWKWK-Int** binding to **GGAGloop RNA**. Shown is the phosphorimage of a 20% denaturing polyacrylamide gel. Structure lanes: RNA only, folded RNA in buffer; AH, alkaline hydrolysis; T1, RNase T1 (G-lane); A, RNase A (C and U lane). Increasing concentrations (0 to 100 μM) of **RevWKWK-Int** were added to **GGAGloop RNA** (0.18 μM) in 10 mM PBS buffer (140 mM Na^+/K^+Cl^-, 1 mM $MgCl_2$, pH 7.4) and 5 ng/μL yeast tRNA. (c) Schematic representation of **WKWK-Int** and **RevWKWK-Int** bound to RNA. N and C indicate the N-terminus and C-terminus of the peptide, respectively.

resin (0.07 mmol scale, 150 mg resin) using standard FMOC solid phase peptide synthesis methodology on an automated peptide synthesizer until the position where FMOC-Lys(ivDde)-OH (0.14 mmol, 2 eq.) was coupled by hand. The peptide was returned to the synthesizer for coupling of the remainder of the natural amino acids. After the βAla-βAla-Arg linker was added, the intercalator portion was manually coupled overnight using HOBT/HBTU (4 eq. each) and DIPEA (8 eq.). The N-terminal Alloc protecting group was deprotected using $Pd(PPh_3)_4$ (1 eq.) and phenylsilane (24 eq.) in dry dichloromethane. The FMOC-Val-OH and BOC-Ser-OH amino acids, respectively, were coupled using HOBT/HBTU and DIPEA (0.4 mmol of each) in DMF. The peptides were fluorescently labeled by first deprotecting the ivDde protecting group with 2% hydrazine in DMF three times for 3 minutes each time. The free amine on the lysine side chain was coupled overnight to 5-(and -6)-carboxytetramethylrhodamine (TAMRA) (0.16 mmol). The BOC group on the N-terminus was used in order to keep the N-terminus protected during the hydrazine deprotection and fluorophore coupling steps. All the peptides were cleaved and deprotected by treating the resin with a (95:2.5:2.5) TFA:TIPS:water mixture and bubbling with N_2 for 3 hours. The peptides were isolated by evaporating the TFA with nitrogen gas, then precipitating the peptide in cold diethyl ether, and then peptide extraction using MilliQ water. The resulting solution was frozen and lyophilized to give a dark pink powder. The peptides were purified using a Waters reverse-phase HPLC system. During purification a C18 column was used, and the peptides were eluted using Standard A (95% water, 5% acetonitrile, 0.1% TFA) and Standard B (95% acetonitrile, 5% water, 0.1% TFA). The masses of the peptides were confirmed using ESI-TOF mass spectrometry (Fig. S8, supplemental information).

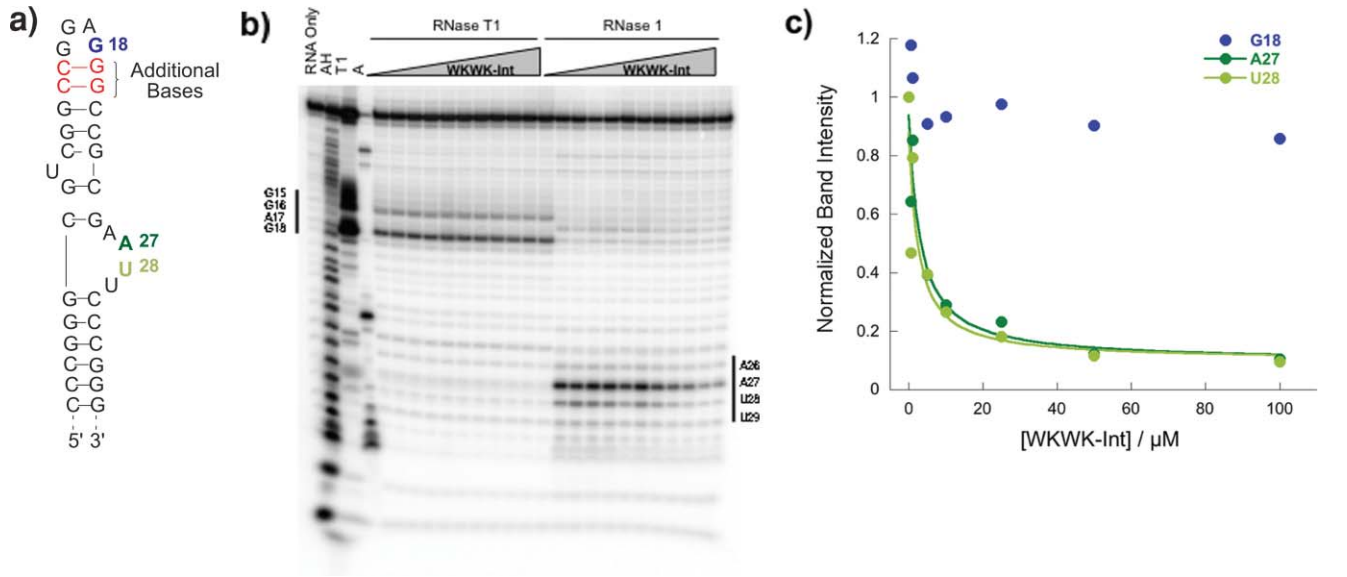

Fig. 6 RNase footprinting assays with an extended RNA, **GGAGext RNA**, with **WKWK-Int**. (a) Sequence and secondary structure of **GGAGext RNA**. The additional bases are highlighted with parentheses. (b) RNase footprinting experiments for **WKWK-Int** binding to **GGAGext RNA**. Shown is the phosphorimage of a 20% denaturing polyacrylamide gel. Structure lanes: RNA only, folded RNA in buffer; AH, alkaline hydrolysis; T1, RNase T1 (G-lane); A, RNase A (C and U lane). Increasing concentrations (0 to 100 μM) of **WKWK-Int** were added to **GGAGext RNA** (0.18 μM) in 10 mM PBS buffer (140 mM Na^+/K^+Cl^-, 1 mM $MgCl_2$, pH 7.4) and 5 ng/μL yeast tRNA. (c) ImageQuant analysis showing the average of two RNase footprinting assays showing the degree of protection at G18 (blue), A27 (dark green), and U28 (light green).

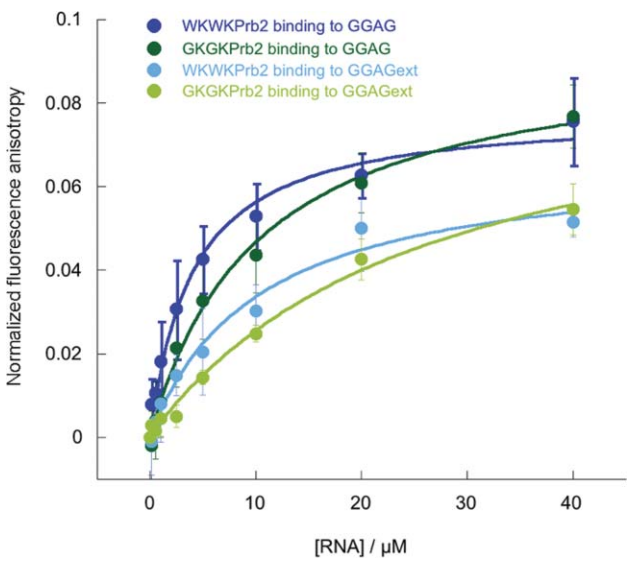

Fig. 7 Comparison of the fluorescence anisotropy binding experiments of TAMRA-labeled heteroconjugates with **GGAGloop RNA** to **GGAGext RNA** or **GGAGloop RNA**. Increasing concentrations of TAMRA-labeled peptides were incubated with the RNA (500 nM) for 30 minutes in 10 mM PBS buffer (140 mM Na^+/K^+Cl^-, 1 mM $MgCl_2$, pH 7.4) at 25 °C. Each curve is an average of 3 or 4 runs.

Secondary structure determination using circular dichroism

Studies were done using an Aviv Model 62DS Circular Dichroism Spectrometer. A wavelength scan (185 nm-260 nm) was done of **WKWK-Int**, **GKGK-Int**, and **GWKWK-Int** in 10 mM sodium phosphate buffer (pH 7.6) at 37 °C in a 0.1 cm cell. The peptide concentration was 100 μM in both cases and the scans were done in triplicate.

Fluorescence anisotropy binding experiments

The RNA sequences were purchased as a purified, lyophilized powder from Integrated DNA Technologies. The RNA was dissolved in DEPC-treated water and annealed by heating to 95 °C for 2 minutes, then slowly cooling to room temperature. The folded RNA solution was separated into smaller aliquots and stored at –20 °C. The peptide-intercalator conjugates were dissolved in DEPC-treated water and the concentration of the solution was determined using UV-Vis (λ_{max}/nm 559 (ε/dm^3 mol^{-1} cm^{-1} 91 000).[24] The binding experiments were done by incubating 0.5 μM TAMRA-labeled peptide-intercalator with increasing concentrations of folded RNA in reaction buffer (10 mM phosphate buffer, 140 mM Na^+/K^+Cl^-, 1 mM $MgCl_2$, pH 7.4) for 30 minutes at room temperature. The anisotropy data were collected at 25 °C in a 1 cm pathlength quartz microcuvette (excited at 548 nm and emission monitored at 580 nm). The anisotropy data were plotted as a function of fluorescence anisotropy *versus* concentration of RNA added. Each of the curves was normalized so that the initial fluorescence anisotropy point equaled zero. The plot was fitted using eqn (1) derived from a previous report,[25] where r is anisotropy, r_0 is initial anisotropy value, r_∞ is the maximum anisotropy, [Pep] is the peptide-intercalator conjugate concentration, x is the concentration of RNA added, K_d is the dissociation constant.

$$r = \left(\left(\frac{\left([\mathrm{Pep}] + x + K_\mathrm{d} \right) \pm \sqrt{\left(-[\mathrm{Pep}] - x - K_\mathrm{d} \right)^2 - 4\left([\mathrm{Pep}]x \right)}}{2[\mathrm{Pep}]} \right) \left(r_\infty - r_0 \right) \right) + r_0 \quad (1)$$

3′-^{32}P RNA labeling

Approximately 10 μg of RNA construct was treated with T4 RNA ligase (2 U/μL), T4 RNA ligase buffer (1X), DMSO (10%), RNase inhibitor (1 U/μL), and ^{32}pCp (0.05 mCi) and incubated at 4 °C overnight. The labeled RNA solution was run through an RNA spin column and loaded onto a 20% denaturing polyacrylamide gel for purification. The labeled RNA was visualized by autoradiography, excised from the gel and eluted overnight with elution buffer (0.5 M NH_4OAc, 1 mM EDTA, 0.1% SDS). After filtration the RNA was precipitated with 95% ethanol, sodium acetate buffer, and linear acrylamide overnight at –20 °C. The RNA was brought up in DEPC-treated water and the concentration was determined by UV absorbance at 260 nm.

RNase footprinting experiments

The labeled RNA was brought up in DEPC-treated water and denatured at 95 °C for 2 minutes and reannealed slowly by cooling to room temperature. The peptide-intercalator ligands were synthesized using the same procedure as above except without the fluorophore label. Instead of inserting an FMOC-Lys(ivDde)-OH residue, an FMOC-Orn(Boc)-OH residue was used. The unlabeled peptide-intercalator conjugates were dissolved in DEPC-treated water and the concentration of the solution was determined using the absorbance of the quinoline molecule (λ_{max}/nm 359 (ε/dm^3 mol^{-1} cm^{-1} 11 700)).[18] The folded RNA (0.18 μM) was incubated with increasing concentrations of the peptide ligands (0 μM, 0.025 μM, 0.1 μM, 0.25 μM, 0.5 μM, 1.0 μM, 5.0 μM, 10.0 μM, 25.0 μM, 50.0 μM, and 100 μM), 5 μg/mL yeast tRNA, and 10 mM PBS buffer (140 mM Na^+/K^+Cl^-, 1 mM $MgCl_2$, pH 7.4) for 30 minutes at room temperature. RNase digestions were done with RNase T1 (0.1 U/μL), RNase 1 (10 U/μL), and RNase V1 (0.01 U/μL) for 5 minutes, 30 seconds, and 1 minute, respectively, and quenched with loading dye. Sequencing lanes were done using unfolded RNA and alkaline hydrolysis buffer, RNase T1, and RNase A (1 μg/mL). Digested RNA and sequencing reactions were heat denatured and loaded onto a 20% denaturing polyacrylamide gel electrophoresis (51 W, 2.5 hours). The gel was visualized by phosphorimaging, and the intensity of the bands was quantified using ImageQuant analysis program. In order to correct the data for differences in loading, the intensity of each band was divided by the intensity of a control lane which is unchanged during the reaction. The data were plotted on Kaleidograph as normalized band intensity *versus* concentration of peptide-intercalator added and fit using eqn (1). In this case, r is the normalized band intensity, r_0 is initial band intensity, r_∞ is band intensity at the maximum peptide-intercalator conjugate concentration, $[RNA]_0$ is the RNA concentration, x is the total concentration of peptide-intercalator conjugate added, K_d is the dissociation constant.

Acknowledgements

This work was supported by funding from the National Institutes of Health, Institute of General Medical Sciences (GM072691). We gratefully acknowledge assistance with the footprinting experiments from Professor Holden Thorp and Dr. Julie Sullivan.

References

1 (*a*) J. R. Thomas and P. J. Hergenrother, *Chem. Rev.*, 2008, **108**, 1171; (*b*) Y. Tor, *ChemBioChem*, 2003, **4**, 998.
2 (*a*) K. Nagai, *Curr. Opin. Struct. Biol.*, 1992, **2**, 131; (*b*) R. C. Deo, J. B. Bonanno, N. Sonenberg and S.K. Burley, *Cell*, 1999, **98**, 835; (*c*) N. Handa, O. Nureki, K. Kurimoto, I. Kim, H. Sakamoto, Y. Shimura, Y. Muto and S. Yokoyama, *Nature*, 1999, **398**, 579; (*d*) S. R. Price, P. R. Evans and K. Nagai, *Nature*, 1998, **394**, 645; (*e*) P. Legault, J. Li, J. Mogridge, L. E. Kay and J. Greenblatt, *Cell*, 1998, **93**, 289; (*f*) C. Oubridge, N. Ito, P. R. Evans, C.-H. Teo and K. Nagai, *Nature*, 1994, **372**, 432.
3 J. Silva and I. Carvalho, *Curr. Med. Chem.*, 2007, **14**, 1101.
4 G. R. Lawton and D. H. Appella, *J. Am. Chem. Soc.*, 2004, **126**, 12762.
5 (*a*) X. Liu, J. R. Thomas and P. J. Hergenrother, *J. Am. Chem. Soc.*, 2004, **126**, 9196; (*b*) J. R. Thomas, X. Liu and P. J. Hergenrother, *J. Am. Chem. Soc.*, 2005, **127**, 12434; (*c*) J. R. Thomas, X. Liu and P. J. Hergenrother, *Biochemistry*, 2006, **45**, 10928.
6 (*a*) Z. Athanassiou, R. L. A. Dias, K. Moehle, N. Dobson, G. Varani and J. A. Robinson, *J. Am. Chem. Soc.*, 2004, **126**, 6906; (*b*) T. C. Leeper, Z. Athanassiou, R. L. A. Dias, J. A. Robinson and G. Varani, *Biochemistry*, 2005, **44**, 12362; (*c*) Z. Athanassiou, K. Patora, R. L. A. Dias, K. Moehle, J. A. Robinson and G. Varani, *Biochemistry*, 2007, **46**, 741; (*d*) V. A. Burns, B. G. Bobay, A. Basso, J. Cavanagh and C. Melander, *Bioorg. Med. Chem. Lett.*, 2008, **18**, 565; (*e*) B. R. McNaughton, P. C. Gareiss and B. L. Miller, *J. Am. Chem. Soc.*, 2007, **129**, 11306.
7 (*a*) S. Hyun, H. J. Kim, N. J. Lee, K. H. Lee, Y. Lee, D. R. Ahn, K. Kim, S. Jeong and J. Yu, *J. Am. Chem. Soc.*, 2007, **129**, 4514; (*b*) A. Pustowka, J. Dietz, J. Ferner, M. Baumann, M. Landersz, C. Konigs, H. Schwalbe and U. Dietrich, *ChemBioChem*, 2003, **4**, 1093; (*c*) C. Raja, J. Ferner, U. Dietrich, S. Avilov, D. Ficheux, J.-L. Darlix, H. de Rocquigny, H. Schwalbe and Y. Mely, *Biochemistry*, 2006, **45**, 9254; (*d*) J. Kawakami, N. Sugimoto, H. Tokitoh and Y. Tanabe, *Nucleosides, Nucleotides Nucleic Acids*, 2006, **25**, 391; (*e*) R. J. Austin, T. Xia, J. Ren, T. T. Takahashi and R. W. Roberts, *J. Am. Chem. Soc.*, 2002, **124**, 10966.
8 (*a*) C. B. Carlson and P. A. Beal, *Bioorg. Med. Chem. Lett.*, 2000, **10**, 1979; (*b*) C. B. Carlson, R. J. Spanggord and P. A. Beal, *ChemBioChem*, 2002, **3**, 859.
9 S. R. Kirk, N. W. Luedtke and Y. Tor, *J. Am. Chem. Soc.*, 2000, **122**, 980.
10 N. W. Luedtke, Q. Liu and Y. Tor, *Biochemistry*, 2003, **42**, 11391.
11 M. Kaiser, M. Sainlos, J.-M. Lehn, S. Bombard and M.-P. Teulade-Fichou, *ChemBioChem*, 2006, **7**, 321.
12 (*a*) C.-H. Wong, M. Hendrix, D. D. Manning, C. Rosenbohm and W. A. Greenberg, *J. Am. Chem. Soc.*, 1998, **120**, 8319; (*b*) D.-R. Ahn and J. Yu, *Bioorg. Med. Chem.*, 2005, **13**, 1177.
13 (*a*) V. Peytou, R. Condom, N. Patino, R. Guedj, A.-M. Aubertin, N. Gelus, C. Bailly, R. Terreux and D. Cabrol-Bass, *J. Med. Chem.*, 1999, **42**, 4042; (*b*) A. Litovchick, A. G. Evdokimov and A. Lapidot, *Biochemistry*, 2000, **39**, 2838.
14 (*a*) S. Hyun, K. H. Lee and J. Yu, *Bioorg. Med. Chem. Lett.*, 2006, **16**, 4757; (*b*) J. Lee, M. Kwon, K. H. Lee, S. Jeong, S. Hyun, K. J. Shin and J. Yu, *J. Am. Chem. Soc.*, 2004, **126**, 1956.
15 Y. Lee, S. Hyun, H. J. Kim and J. Yu, *Angew. Chem., Int. Ed.*, 2007, **46**, 1.
16 (*a*) S. M. Butterfield, W. J. Cooper and M. L. Waters, *J. Am. Chem. Soc.*, 2005, **127**, 24; (*b*) A. L. Stewart and M. L. Waters, *ChemBioChem*, 2009, **10**, 539.
17 (*a*) S. M. Butterfield and M. L. Waters, *J. Am. Chem. Soc.*, 2003, **125**, 9580; (*b*) S. M. Butterfield, M. M. Sweeney and M. L. Waters, *J. Org. Chem.*, 2005, **70**, 1105.

18 M. Krishnamurthy, B. D. Gooch and P. A. Beal, *Org. Biomol. Chem.*, 2006, **4**, 639.
19 L. L. Cline, unpublished work.
20 R. N. De Guzman, Z. R. Wu, C. C. Stalling, L. Pappalardo, P. N. Borer and M. F. Summers, *Science*, 1998, **279**, 384.
21 W. J. Cooper and M. L. Waters, *Org. Lett.*, 2005, **7**, 3825.
22 T. Hermann and D. J. Patel, *Structure*, 2000, **8**, R47.
23 (*a*) B. D. Gooch and P. A. Beal, *J. Am. Chem. Soc.*, 2004, **126**, 10603; (*b*) B. D. Gooch, M. Krishnamurthy, M. Shadid and P. A. Beal, *ChemBioChem*, 2005, **6**, 2247.
24 Extinction coefficient provided by Integrated DNA Technologies, www.idtdna.com.
25 (*a*) Y. Wang and R. R. Rando, *Chem. Biol.*, 1995, **2**, 281; (*b*) Y. Wang, K. Hamasaki and R. R. Rando, *Biochemistry*, 1997, **36**, 768.

